Time-resolved magnetic domain imaging by X-ray photoemission electron microscopy

J. Vogel,[1] W. Kuch,[2] M. Bonfim,[3] J. Camarero,[1] F. Offi,[2] Y. Pennec,[1]
K. Fukumoto,[2] J. Kirschner,[2] A. Fontaine,[1] and S. Pizzini[1]

[1]*Laboratoire Louis Néel, CNRS, B.P.166, F-38042 Grenoble, France*
[2]*Max-Planck-Institut für Mikrostrukturphysik, Weinberg 2, D-06120 Halle, Germany*
[3]*Departamento de Engenharia Elètrica, Universidade do Paraná, CEP 81531-990, Curitiba, Brazil*

(Dated: September 17, 2002)

We have performed nanosecond time-resolved magnetic X-ray photoemission electron microscopy (X-PEEM) on the permalloy layer of a $Ni_{80}Fe_{20}$ (5nm)/Cu(10nm)/Co(5nm) trilayer deposited on Si(111). The measurements were performed in the pump-probe mode, where a magnetic pulse from a microcoil was synchronised with the X-ray photon bunches delivered by the BESSY synchrotron in single bunch mode. Images could be acquired during and after the 20 ns long and 80 Oe high field pulses. The nucleation and subsequent growth of reversed domains in the permalloy could be observed, demonstrating the feasibility of element selective and time-resolved domain imaging using X-PEEM.

PACS numbers: 75.70.Ak, 75.60.Jk, 07.85.Qe, 75.50.Bb

Magnetization reversal dynamics at nanosecond timescales is an important subject for many technological applications of magnetic materials. In magnetic recording industry, the fast magnetization reversal in storage media and read heads is primordial to guarantee a high data transfer rate. Read and write speeds are today of the order of 600 MHz and are not limited by the magnetization reversal times. As these times will evolve towards the GHz regime, limitations due to magnetization reversal speeds can be expected.

In order to improve the performance of materials for fast magnetic applications, the fundamental understanding of magnetization reversal processes at high speed should be improved. Several studies of sub-nanosecond magnetization reversal in thin films and nanosystems have been carried out recently. The most successful investigations use time-resolved magneto-optical microscopy [1–3]. Femto-second lasers synchronized with ps-long magnetic pulses can be used in pump-probe mode to get access to the evolution of the magnetic domain structure of microstructures with sub-micron resolution [1].

The time structure of synchrotron radiation can also be used to study magnetization reversal dynamics [4, 5], and in combination with the element selectivity of X-ray Magnetic Circular Dichroism (XMCD) this can be done independently for each magnetic layer of complex heterostructures. Our first time-resolved XMCD measurements on magnetic spin valves [5] have demonstrated that the strength of the coupling between the soft and the hard magnetic layers can be different in quasi-static and nanosecond regimes. We have attributed this behavior to the difference in magnetization reversal processes in the two regimes. While propagation of domain walls dominates in the quasi-static regime, nucleation of reversed domains dominates at high speeds. In order to improve the understanding of the dynamic coupling in multilayer systems, a time-resolved imaging technique able to probe the different magnetic layers independently is desirable. For this purpose, we have developed the first time-resolved X-ray Photoemission Electron Microscopy (X-PEEM) measurements in pump-probe mode. This was done by extending the set-up developed for the time-resolved XMCD measurements at the European Synchrotron Radiation Facility (ESRF) [5, 6]. X-PEEM combines photoemission electron microscopy with excitation by circularly (or linearly) polarized x-ray synchrotron radiation tuned to atomic absorption edges. Secondary electrons emitted at the sample surface are used to create a magnified image of the sample, the intensity of which is proportional to the local absorption. For circular polarization, magnetic contrast arises from the dependence of the absorption on the relative orientation of local magnetization and light polarization vector (XMCD). Linearly polarized X-rays provide a sensitivity to the orientation (perpendicular or parallel) of the magnetization axis with respect to the polarization vector of the light (X-ray Magnetic Linear Dichroism or XMLD). While XMCD is only sensitive to ferromagnetic order, XMLD can also probe antiferromagnetic order [7, 8]. The element selectivity of x-ray absorption allows the domain patterns in different ferromagnetic layers separated by a non-magnetic or an anti-ferromagnetic layer to be observed separately [9–11], as well as the correlation and interaction between them. X-PEEM adds spatial resolution to the time resolution and chemical selectivity of pump-probe XMCD measurements.

Our time-resolved X-PEEM measurements were performed at the UE56/2-PGM2 helical undulator beamline of BESSY II in Berlin. Circularly polarized X-rays emitted by the fifth harmonic of the undulator (degree of circular polarization about 80%) were used. The set-up of the electrostatic photoelectron emission microscope (Focus IS-PEEM) is identical to that described in previous publications [9]. The spatial resolution provided by this

set-up depends on the experimental conditions and instrument settings, and in our case was selected to be of the order of 1 μm.

In single bunch mode operation of BESSY, photon bunches are emitted with a frequency of 1.25 MHz (800 ns separation between bunches). Like time-resolved XMCD, the X-PEEM measurements were performed in pump-probe mode, by synchronizing the applied magnetic field pulses with the x-ray photon bunches. Magnetization reversal dynamics is then studied as a function of time, during and after the magnetic pulse, by changing the delay between magnetic and photon pulses. As it is always the case for pump-probe measurements, the magnetization reversal processes have to be both reversible *and* reproducible in order to be observed.

Measurements were carried out on the permalloy layer of a $Ni_{80}Fe_{20}$(5nm)/Cu(10nm)/Co(5nm) spin valve-like trilayer deposited on a step-bunched Si(111) substrate. The preparation and static magnetic properties of this sample have been described in Ref. [15]. The terraces of the substrate induce an in-plane uniaxial anisotropy in the magnetic layers, parallel to the steps. The sample was set at the inner surface of a double stripline copper coil, made of 12.5 μm thick Cu foil. The angle of incidence of X-rays on the sample was 60° from the surface normal. Magnetic pulses were provided by sending a fast current pulse through a low impedance coaxial cable made of two 12.5μm thick and 15mm wide copper strips connected to the microcoil. The strong currents (up to 30 A) needed to reverse the magnetization of the permalloy layer in dynamic conditions were provided by a current driver [6, 14] based on fast power MOSFET transistors, located outside the vacuum chamber. At the used repetition rate, up to 50 ns long magnetic pulses with 8 ns risetime could be obtained. Due to the deviation of the relatively slow secondary electrons by the applied magnetic field, images taken during the magnetic field pulse appear shifted with respect to the image taken without field. However, as the field is localized close to the sample, the shift is relatively small, at most 10-15 μm for a field of view of 120 μm.

An important issue for the generation of sufficiently high magnetic fields is to limit the power dissipation in the microcoil and in the pulse power supply. This was achieved by lowering the repetition rate of the pulses by integer factors with respect to the one of the synchrotron. For the measurements presented here a repetition rate of 312.5 kHz was used. The single-bunch marker signal passing through a 1/4 electronic frequency divider was used to trigger the power supply. Therefore, only one magnetic pulse was provided for every four photon pulses. The other three photon pulses would contribute to the PEEM image by increasing the non-magnetic background. To avoid this, electrons emitted by the photon pulses that are not following a magnetic pulse were blanked out using a commercially available retarding field electron energy analyzer [16]. This is located before the

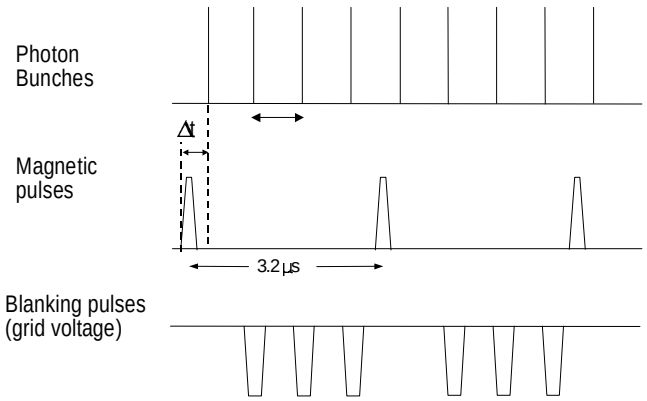

FIG. 1: Photon pulses (top) of about 100 ps length arrive on the sample every 800 ns. A magnetic pulse is given every 3.2 microseconds (middle), with a width of 20 ns and a delay Δt with respect to one of the photon pulses. For the other three photon pulses, a negative pulse of 80V and 80 ns width is given to the grid of the PEEM (bottom) to block most of the secondary electrons.

imaging unit, and acts like a high pass imaging energy filter [17]. Voltage pulses of -80 V height and 80 ns width were provided to the retarding grid of the analyzer by the gated operation of a HP214B pulse generator, synchronized to the photon bunches not associated to a magnetic pulse. Electrons with a kinetic energy of less than 80 eV, which make up for more than 95% of the image intensity, are therefore suppressed. The overall scheme of the synchronization is given in Figure 1. The delay Δt between photon and magnetic pulse was set using a Stanford Research Systems DG535 delay generator, which also triggered the voltage pulses to the electron analyzer.

In Figure 2 we show X-PEEM images of the $Ni_{80}Fe_{20}$/Cu/Co trilayer measured for different delays between field and photon pulses. In the images, the easy magnetization axis is vertical, and the field pulses are applied parallel to this axis. The photon energy was tuned to the maximum of the Fe L_3 absorption white line (707 eV), providing sensitivity to the permalloy layer only. The five images were taken with delays of 13, 15, 17, 20 and 22 nanoseconds after the maximum of the field pulse. The images were obtained at room temperature, using the asymmetry (difference divided by sum) of two images taken with opposite photon helicity. The contrast is due to the difference in absorption between regions of the sample which have their magnetization parallel and anti-parallel to the direction of the incoming X-rays.

The first positive pulse was used to saturate the permalloy layer, while the dynamics was monitored during the negative and subsequent positive overshoot. Images were acquired over about three minutes for each helicity of the incoming X-rays, meaning that each asym-

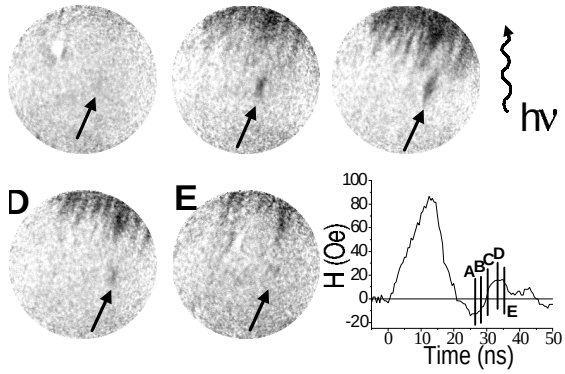

FIG. 2: Magnetic PEEM domain images of a NiFe layer, taken 13, 15, 17, 20 and 22 ns after the maximum of a 80 Oe field pulse. The shape of the pulse as well as the time position with respect to the pulse are given below the images. The arrows indicate a nucleated and subsequently expanding reversed domain. The direction of the incoming photons is also indicated.

metry image corresponds to an average over more than 100 million magnetic pulses. The contrast of the images is limited, because the nucleation of reversed domains for each magnetic pulse is probably not completely reproducible, but also because the nucleated domains are small with respect to the resolution of the image (about 1 μm). In the first image, the nucleation sites which have been generated during the rise of the negative pulse are weakly visible and the clearest of them has been marked with an arrow. In the second and third images the nucleated sites have grown through propagation of the formed domain walls and the contrast becomes larger due to the larger domains. The larger amount of nucleated reverse domains in the top of the image indicates that the field is not completely homogeneous. In the third image, several small, well separated domains can be seen. The domains disappear during the positive overshoot. These images show clearly that the reversal for these short pulses takes place through nucleation of several reversed domains during the rise of the pulse and subsequent propagation of the formed domain walls. This experimentally proves that for these short, strong pulses the reversal is dominated by nucleation processes, and is coherent with our explanation for the disappearance of the orange-peel coupling in these samples [5, 18].

These first results show the feasibility of time-resolved X-PEEM measurements. They open the way for nanosecond resolved studies of magnetization dynamics with layer selectivity and spatial resolution. With the improvements in both synchrotron X-ray sources and X-PEEM microscopes, picosecond time resolution and spatial resolution down to 10 nm can be foreseen in the near future.

J.C. acknowledges the European Union for a Marie-Curie Fellowship. We thank F.Petroff and A. Encinas for sample preparation. Financial support by BMBF (no. 05KS1EFA6) and EU (BESSY-EC-HPRI Contract No. HPRI-1999-CT-00028) is gratefully acknowledged.

[1] B.C. Choi, G.E. Ballentine, M. Belov, W.K. Hiebert, and M.R. Freeman, Phys.Rev.Lett. **86**, 728 (2001); B.C. Choi, G.E. Ballentine, M. Belov, and M.R. Freeman, Phys.Rev.B **64**, 144418 (2001).

[2] A. Kirilyuk, J. Ferré, J. Pommier, and D. Renard, J.Magn.Magn.Mater. **121**, 536 (1993).

[3] R.P. Cowburn, J. Ferré, S.J. Gray, and J.A.C. Bland, Phys.Rev.B **58**, 11507 (1998).

[4] F. Sirotti, R. Bosshard, P. Prieto, G. Panaccione, L. Floreano, A. Jucha, J.D. Bellier, and G. Rossi, J.Appl.Phys. **83**, 1563 (1998); F. Sirotti, S. Girlando, P. Prieto, L. Floreano, G. Panaccione, and G. Rossi, Phys.Rev.B **61**, R9221 (2000).

[5] M. Bonfim, G. Ghiringhelli, F. Montaigne, S. Pizzini, N.B. Brookes, F. Petroff, J. Vogel, J. Camarero, and A. Fontaine, Phys.Rev.Lett. **86**, 3646 (2001).

[6] Marlio Bonfim, Ph.D.Thesis, Université Joseph Fourier, Grenoble, 2001.

[7] D. Alders, L.H. Tjeng, F.C. Voogt, T. Hibma, G.A. Sawatzky, C.T. Chen, J. Vogel, M. Sacchi, and S. Iacobucci, Phys.Rev.B **57**, 11623 (1998).

[8] H. Ohldag, A. Scholl, F. Nolting, S. Anders, F.U. Hillebrecht, and J. Stöhr, Phys.Rev.Lett. **86**, 2878 (2000); H. Ohldag, T.J. Regan, J. Stöhr, A. Scholl, F. Nolting, J. Lüning, C. Stamm, S. Anders, and R.L. White, Phys.Rev.Lett. **87**, 247201 (2001).

[9] W. Kuch, R. Frömter, J. Gilles, D. Hartmann, Ch. Ziethen, C.M. Schneider, G. Schönhense, W. Swiech, J. Kirschner, Surf.Rev.Lett. **5**, 1241 (1998).

[10] G. Schönhense, J.Phys.: Condens. Matter **11**, 9517 (1999).

[11] W. Kuch, X. Gao, and J. Kirschner, Phys.Rev.B **65**, 064406 (2002).

[12] B.T. Thole, P. Carra, F. Sette, and G. van der Laan, Phys.Rev.Lett. **68**, 1943 (1992); P. Carra, B.T. Thole, M. Altarelli, and X. Wang, Phys.Rev.Lett. **70**, 694 (1993).

[13] J. Stöhr, H.A. Padmore, S. Anders, T. Stammler, and M.R. Scheinfein, Surf.Rev.Lett. **5**, 1297 (1998).

[14] K. Mackay, M. Bonfim, D. Givord, and A. Fontaine, J.Appl.Phys. **87**, 1996 (2000).

[15] A. Encinas, F. Nguyen Van Dau, M Sussiau, A. Schuhl, and P. Galtier, Appl.Phys.Lett. **71**, 3299 (1997).

[16] Focus Imaging Energy Filter (IEF), Omicron Nanotechnology GmbH.

[17] W. Kuch, L.I. Chelaru, F. Offi, M. Kotsugi, and J. Kirschner, submitted to J.Vac.Sci.Technol. B.

[18] Y. Pennec et al., to be published